CrossMark

METHOD

Diffuse Intrinsic Pontine Gliomas Exhibit Cell Biological and Molecular Signatures of Fetal Hindbrain-Derived Neural Progenitor Cells

Yu Sun[1] · Cheng Xu[1] · Changcun Pan[1] · Xin Chen[1] · Yibo Geng[1] ·
Yuliang Wu[1] · Peng Zhang[1] · Wenhao Wu[1] · Yu Wang[1] · Deling Li[1] ·
Zhen Wu[1] · Junting Zhang[1] · Qiaoran Xi[2] · Liwei Zhang[1]

Abstract Diffuse intrinsic pontine glioma (DIPG) is the main cause of brain tumor-related death among children. Until now, there is still a lack of effective therapy with prolonged overall survival for this disease. A typical strategy for preclinical cancer research is to find out the molecular differences between tumor tissue and para-tumor normal tissue, in order to identify potential therapeutic targets. Unfortunately, it is impossible to obtain normal tissue for DIPG because of the vital functions of the pons. Here we report the human fetal hindbrain-derived neural progenitor cells (pontine progenitor cells, PPCs) as normal control cells for DIPG. The PPCs not only harbored similar cell biological and molecular signatures as DIPG glioma stem cells, but also had the potential to be immortalized by the DIPG-specific mutation H3K27M *in vitro*. These findings provide researchers with a candidate normal control and a potential medicine carrier for preclinical research on DIPG.

Keywords Diffuse intrinsic pontine glioma · Neural progenitor cells · Immortalization · H3K27M · Senescence

Introduction

Diffuse intrinsic pontine glioma (DIPG) is the main cause of brain tumor-related death among children, with a median survival of $\sim$ 10 months and 2-year overall survival $< 10\%$ [1, 2]. Because of the infiltrative characteristic of the tumor and the essential physiological functions of the pons, surgical management is not an option. Although biopsy and primary cell culture techniques have provided access to DIPG cells for preclinical research [3], there is still a barrier to obtaining para-tumor normal control tissue to dissect the molecular differences between DIPG and normal cells. Neural stem cells and neural progenitor cells (NPCs) participate in tissue development and repair. The developmental programs re-emerge in cancer stem cells to support the development and progressive growth in glioblastoma [4]. Previously, investigators derived early NPCs from human embryonic stem cells to model DIPG [5], which made it possible to use NPCs as normal control for DIPG. However, the efficiency of the dual smad inhibition protocol for converting human embryonic stem cells to NPCs is 80% [6], while the NPC populations differ between cerebral cortex and brainstem [3]. Furthermore, transcriptome analysis of different regions in the brain has revealed that region and age contribute most to the global differences in gene expression in the central nervous system [7]. All these considerations make it urgent to find normal control cells appropriate for preclinical research on DIPG. Aborted early human embryos provide a resource for obtaining hindbrain neuroepithelial stem cells that retain progenitor characteristics and have a high neurogenic capacity [8]. In this research, we report a new method to establish primary neural progenitor cell lines from the hindbrain of aborted human embryos and demonstrate that these cells share

✉ Liwei Zhang
  Zhangliweittyy@163.com

1 Department of Neurosurgery, Beijing Tiantan Hospital, Capital Medical University, Beijing 100070, China

2 Ministry of Education Key Laboratory of Protein Sciences, School of Life Sciences, Tsinghua University, Beijing 100084, China

biological features with DIPG cells. This provides researchers with a candidate normal control for DIPG cells with which to dissect the molecular differences between tumor and normal cells.

Materials and Methods

Ethics Statement

All experiments with human tissues were performed with ethical approval of the Institutional Review Board of Beijing Tiantan Hospital Affiliated with Capital Medical University (Licenses KY2014-021-02 and KY 2018-042-02). All human tissues were obtained with informed consent.

Primary DIPG Cell Lines and Xenograft Mouse Model

Tumor tissues were obtained from treatment-naive DIPG patients following surgical or biopsy procedures in Beijing Tiantan Hospital. Sanger sequencing of the H3F3A/HIST1H3B genes was performed for all the established primary DIPG cell lines and their corresponding tumor tissues. The protocol to establish primary DIPG cell line was as described previously [9]. The primary DIPG cells were transfected with lentivirus containing luciferase-GFP, and GFP-positive cells were enriched by fluorescence-activated cell sorting (FACS). 10^5 DIPG cells were suspended in 5 μL phosphate-buffered saline (PBS), and injected into the pons of 4-week-old female immunodeficient NSG (NOD scid gamma) mice (Beijing Biocytogen Co., Ltd). IVIS lumina II (PerkinElmer) living images were captured every week to monitor tumor growth. MRI images were taken in a 7.0-T magnet (Bruker, Germany) to show the orthotopic tumor in the pons.

Primary Fetal Neural Progenitor Cells

Hindbrain and cortex were isolated from aborted early human embryos (weeks 9–12) after pharmaceutical termination of pregnancy. The establishment of cell lines was as described previously [8]. Fetal hindbrain and cortex were dissected in Dulbecco's modified Eagle's medium (DMEM; Gibco, Carlsbad, CA) with the meninges removed. The tissues were cut into pieces, incubated in DMEM supplemented with papain (20 units/mL; Worthington) and DNase I (5 Kunitz units/mL; Sigma, St. Louis, MO) at 37 °C for 30 min, pipetted up and down every 10 min until a single-cell suspension was formed, and then centrifuged at 300 g for 5 min. The cell pellet was washed twice with DMEM, then the cells were propagated in 6-well plates coated with Matrigel (4–12 h at 37 °C, 1%, BD, Bedford, MA). To enrich the NPCs, after the first passage, the cells were plated in uncoated 6-well plates (Excellbio, Shanghai, China). Neurospheres floating in the medium were isolated three days after plating and cells attached to the bottom of the plate were discarded.

Cell Propagation and Passaging

DIPG cells were plated in Matrigel-coated 6-well plates in serum-free medium containing DMEM, B27 (50 ×; Gibco), N2 (100 ×; Gibco), penicillin/streptomycin (100 ×; Gibco), basic fibroblast growth factor (20 ng/mL), epidermal growth factor (20 ng/mL), and platelet-derived growth factor-AB (PDGF-AB; 20 ng/mL) (Peprotech). NPCs derived from cortex (cortex progenitor cells, CPCs) or hindbrain (PPCs) were propagated in the same medium without PDGF-AB supplement. Half of the medium was changed every 2–3 days to allow culture conditioning and passaged every 3–4 days using 0.05% trypsin for 1–2 min. Digestion was terminated with Defined Trypsin Inhibitor(DTI, Gibco). Cells were washed with DMEM and centrifuged at 300 g for 5 min. The cell pellet was re-suspended in the culture medium at $3–5 \times 10^5$ cells/well to obtain a monolayer. All cultures were routinely tested for mycoplasma.

Western Blot and RT-qPCR

For whole-cell extract analyses, the cells were lysed with 10% SDS lysis buffer. Histone extraction was performed as previously described [10]. The primary antibodies used were anti-H3K27M (Millipore, Darmstadt, Germany), anti-H3K27me3 (active motif), and anti-H3 (Abcam, Cambridge, MA).

RNA was extracted using a total RNA purification kit (Genemark). Reverse transcription was performed using the High Capacity cDNA Reverse Transcription Kit (Invitrogen) and real-time qPCR was carried out using $2 \times$ Maxima SYBR Green qPCR Master Mix (Thermo Scientific).

Sphere Formation Assay

DIPG cells, PPCs, and CPCs were plated on low-attachment 96-well plates (Corning) at 1000 cells/well in 100 μL culture medium. For drug treatment assays, 100 nmol/L or 400 nmol/L panobinostat or 0.1% DMSO was administered the day after seeding, then 25 μL of medium was added in each well every 3 days. After 10 days in culture, cells in each well were photographed.

218

Neurosci. Bull. April, 2019, 35(2):216–224

Senescence-Associated-β-Galactosidase Staining

Cells grown on Matrigel-coated 12-well plates were stained with a senescence-associated β-galactosidase staining kit (Beyotime, Shanghai, China) as described by the manufacturer.

In Vitro Cell Viability and Growth Curves

To generate growth curves, cells were plated at 5,000 cells/well in 15 wells of 96-well plates. Viability was then measured using the Cell Titer Glo assay (Promega, Madison, WI). The luminescence values of 3 wells were recorded every two days from days 0 to 8. To normalize the cell numbers between different cell lines, each luminescence value was divided by the luminescence value on day 0. The ratios were calculated to generate the growth curves.

Ki67 Staining and Cell-Cycle and Flow Cytometry Analysis

Cells were harvested, washed with PBS, and fixed in 70% ethanol at 4 °C overnight. For Ki67 staining, cells were incubated in 0.05% Triton X-100 at 4 °C for 30 min, and stained with Ki-67-PE antibody (eBioscience, San Diego, CA). The percentage of Ki67-positive cells was analyzed by flow cytometry (BD FACS Calibur, Sparks, MD). For cell-cycle distribution analysis, cells were suspended in PBS containing 40 mg/mL propidium iodide (PI) and 100 mg/mL RNase A, and incubated at 37 °C for 30 min. The cell cycle was analyzed by flow cytometry and the data were analyzed using Modfit software (Verity Software House, Topsham, ME).

Apoptosis Analyses

Cells were harvested and stained using the Annexin V-FITC Apoptosis Detection Kit as described by the manufacturer (Beyotime) . FACS analysis was performed after staining to assess the proportion of cells undergoing apoptosis. The data were analyzed using FlowJo software (FlowJo, LLC, Ashland, OR).

Statistical Analyses

Graphpad prism 6 was used for statistical analysis. One-way analysis and Student's t-test were used to determine the significance of differences between groups. $P < 0.05$ was considered to be statistically significant.

Results

DIPG Glioma Stem Cells were Enriched in Patient-Derived Primary DIPG Cell Lines

DIPG tissue samples were obtained from treatment-naïve patients who underwent stereotactic or open biopsy procedures. Primary DIPG cell lines were established as previously described (magnetic resonance imaging and clinical data are shown in Fig. 1A) [9]. The DIPG cells cultured in serum-free stem-cell medium formed neurospheres on the low-attachment plates, similar to NSCs [11] (Fig. 1B). After single-cell isolation by flow cytometry in 96-well plates, a single cell propagated to form a single colony with a probability of 1/15 (data not shown). The DIPG cells were then implanted into the pons of immunodeficient NSG mice. As early as 7 days after implantation, IVIS imaging analyses revealed DIPG tumor growth. MRI imaging of the mouse models and pathological sections showed typical infiltrative high-grade gliomas in the pons (Fig. 1C). Furthermore, we extracted mRNA samples from both the patient tumor and mouse xenograft tumor tissue. After reverse transcription and PCR amplification of H3F3A, Sanger sequencing revealed the same H3.3K27M mutation, which is a driver mutation in DIPG [12]. These results suggested that cancer stem cells, which had the potential to propagate in vitro and form xenograft tumors in immune-deficient mice, were enriched in the primary cell lines derived from DIPG patients.

Validation of the Feasibility of PPCs as Normal Control Cells for DIPGs

We established primary cell lines from the brain tissues obtained from aborted human fetuses. To validate the feasibility of these cells as normal control cells for DIPG cells, we compared the biological behavior, molecular profiling, and sensitivity to DIPG-specific drugs between fetal NPCs and DIPG cells, and demonstrated the possibility of transforming PPCs with DIPG-specific oncogenes.

Neural Progenitor Cells Derived from Human Fetal Cortex and Hindbrain Share Characteristics with Glioma Stem Cells

The progenitor cells derived from cortex and the hindbrain formed neurospheres similar to the cancer stem cells derived from primary DIPG cell lines (Fig. 2A). In Matrigel-coated culture plates, the cells attached to the bottom and formed rosette-like structures, which is a typical behavior of neuroepithelial progenitors [13] (Fig. 2B). The growth rates of PPCs and CPCs were
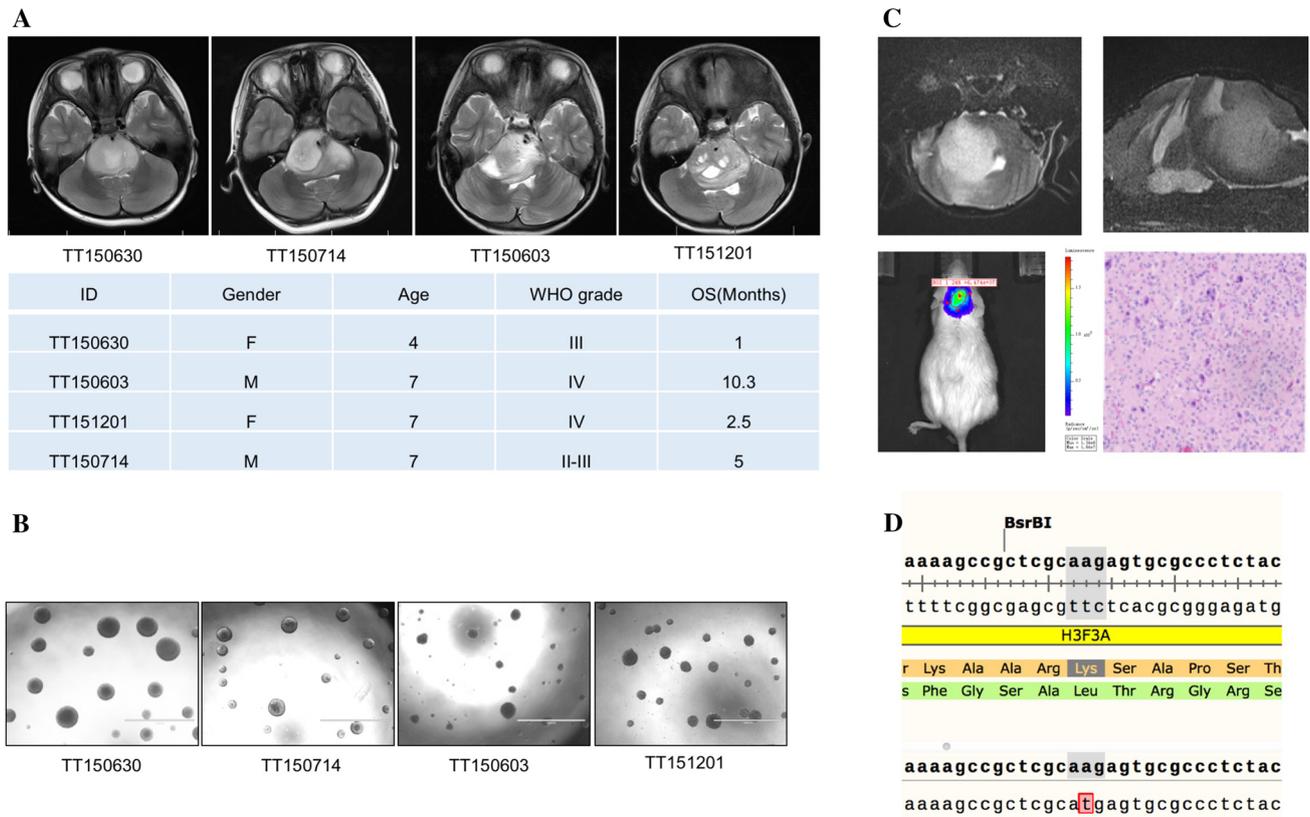
A

ID	Gender	Age	WHO grade	OS(Months)
TT150630	F	4	III	1
TT150603	M	7	IV	10.3
TT151201	F	7	IV	2.5
TT150714	M	7	II-III	5

B

C

D

Fig. 1 Patient-derived primary DIPG cell lines were enriched with cancer stem cells. **A** Upper panel, MRI images of DIPG patients showing the infiltrative characteristics of tumors in the pons. Lower panel, clinical data of the patients. **B** Primary cell lines were established from the patient tumor samples. In the low-attachment culture dishes the cells formed neurospheres (scale bars, 1 mm). **C** MRI imaging (upper panels) and a pathological section (lower right) of the DIPG mouse model revealing the infiltrative feature of the tumors similar to their human counterpart. Lower left, IVIS image of a living mouse model showing an orthotopic tumor in the pons. **D** Sanger sequencing data of H3F3A in PCR samples from both the patient tumor and mouse xenograft cDNA identified the same somatic mutation of H3.3K27M.

similar to DIPG cells *in vitro* (Fig. 2C). Ki67 staining and flow cytometric analysis of the PPCs, CPCs, and DIPG cells demonstrated that the percentage of Ki67-positive cells was similar among these cells (Fig. 2D, left), which is consistent with the growth rate analysis *in vitro*. The G0/ G1, G2, and S phase distributions were similar among these cells (Fig. 2D, right). Annexin V and PI co-staining and flow cytometry revealed no significant difference among these cells (Fig. 2E). Altogether, these results revealed that DIPG cells displayed biological behavior similar to CPCs and PPCs derived from human fetal brain.

Molecular Profiling and Drug Sensitivity Among DIPGs, PPCs, and CPCs

The neural stem-cell markers Sox2, Olig2, Nestin and CD133 are expressed by glioma stem cells [14]. On the contrary, many lineage-specific differentiation markers expressed by terminally-differentiated neural stem cells are also expressed by glioblastoma cells, which reveals a hierarchy among heterogeneous glioblastoma cell populations [15]. In the context of DIPG, the putative cell of origin and the linage specificity are different from adult hemispheric glioblastoma [3]. To profile the molecular landmarks and the lineage specificity among DIPG cells, PPCs, and CPCs, we used RT-PCR to analyze the relative mRNA levels of the stemness and differentiation markers. Among DIPG cells, the expression of these markers varied dramatically. This may be explained by the different cells of origin of the different DIPG cell lines. In PPCs and CPCs, the expression levels of these markers varied between the upper and lower limits of DIPG cells (Fig. 3A). To compare the drug sensitivity between DIPGs, PPCs, and CPCs, we chose panobinostat as the candidate drug, which has known therapeutic efficacy both *in vitro* and in DIPG mouse models [16]. Sphere-forming assays showed that DIPG cells, PPCs, and CPCs had similar sensitivity to panobinostat (Fig. 3B). Therefore, DIPGs, PPCs, and CPCs have similar molecular profiling and sensitivity to targeted therapies.
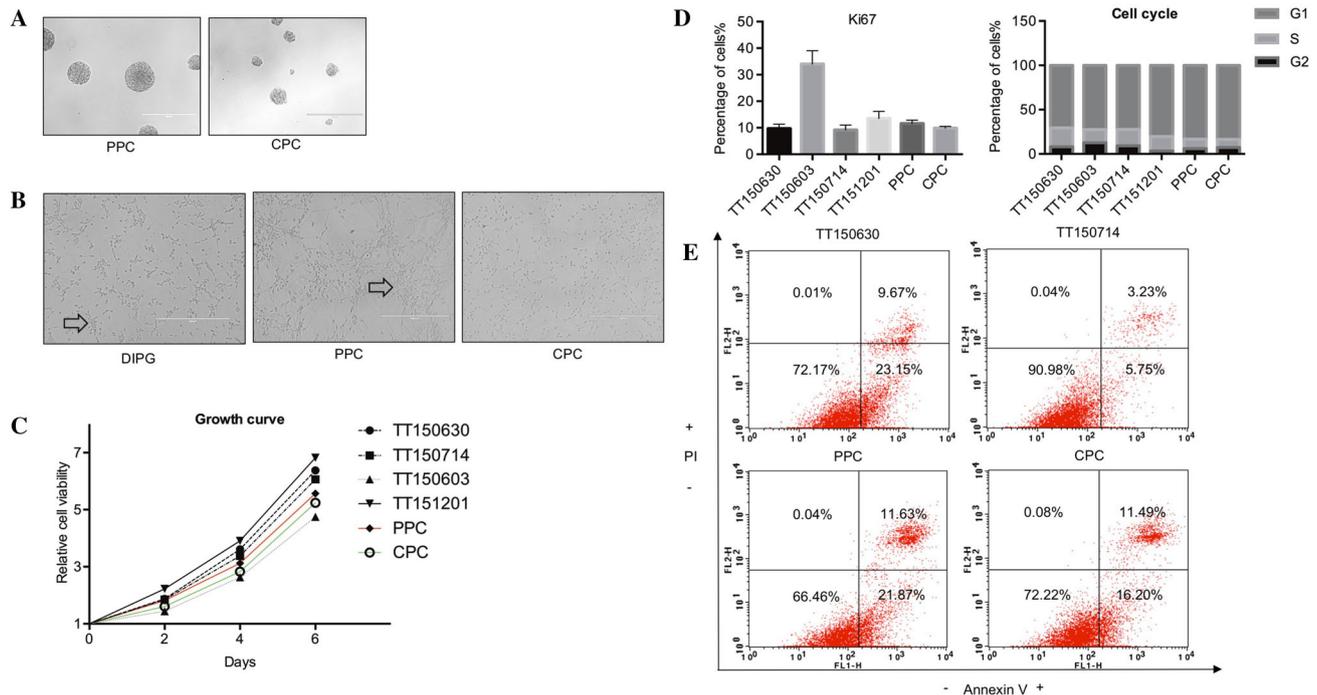
Fig. 2 PPCs and CPCs derived from fetal brain have characteristics similar to DIPG cells. **A** Both PPCs and CPCs cultured in low-attachment dishes with stem-cell medium formed neurospheres (scale bars, 400 μm). **B** PPCs cultured in Matrigel-coated dishes attached to the bottom and formed rosette-like structures (arrows), which were not observed in CPCs (scale bars, 400 μm). **C** Growth rates of the DIPG cells, PPCs, and CPCs as recorded by the Cell-Titer-Glo assay (values normalized to those on day 0). **D** Left, Ki67 staining and flow cytometric analysis showing that the proliferation of PPCs and CPCs was similar to DIPG cells. Right, PI staining and flow cytometric analysis showing that the cell-cycle distribution of CPCs and PPCs was similar to DIPG cells. **E** Annexin V and PI co-staining and flow cytometry demonstrating that the apoptotic population of PPCs and CPCs was similar to DIPG cells (TT150630, TT150603, TT150714 and TT151201 were patient-derived primary DIPG cell lines).

Fetal Brain-Derived CPCs and PPCs Demonstrated Senescence After Long-Term Passaging

The *in vitro* propagation of neural stem cells raises the problem of aging. The CPCs and PPCs derived from fetal brain had the same problem. After 20 passages, their growth rates slowed (Fig. 4A). Meanwhile, the Ki67-positive population shrank compared to early passages (Fig. 4B). PI staining and flow cytometric analysis showed a decreased S-phase population and increased G1-phase cells, revealing G1-S arrest (Fig. 4C). Furthermore, we checked the induction of senescence-associated-β-galactosidase (SA-β-Gal) activity. As the number of passages increased, the percentage of SA-β-Gal-positive cells increased, and flat and enlarged PPCs and CPCs were observed, indicating cell senescence [17]. However, after long-term passaging of DIPG cells, there was no clear phenotype of senescence (Fig. 4D). Therefore, compared to normal NPCs, the cancerous cells had the potential to resist senescence after long-term propagation *in vitro*.

Fetal Hindbrain-Derived PPCs Transformed by DIPG-Specific H3K27M Mutation Became Resistant to Senescence

H3K27M is an important driver mutation in the pathogenesis of DIPG; it decreases the global H3K27me3 distribution on the genomic scale [12]. Oncogene *v-Myc*, which has been used for the immortalization of human-derived NPCs *in vitro* [18], is over-expressed in DIPG cells with H3K27M, while therapy targeting this mutation decreases the expression of myc [19]. Here, we asked whether the onco-mutation H3K27M can be used to immortalize CPCs or PPCs *in vitro*. To answer this question we established cell lines by the ectopic over-expression of H3K27M coding sequence in CPCs and PPCs. The expression of H3K27M was confirmed by Western blotting, which showed the presence of H3K27M mutant protein and decreased H3K27me3 modification compared to cells expressing empty vector (Fig. 5A). After long-term passaging for > 20 passages, the PPCs transformed with H3K27M showed lower SA-β-Gal activity than the empty vector (Fig. 5B). However, H3K27M-transformed CPCs did not survive to > 20 passages. Furthermore, in the
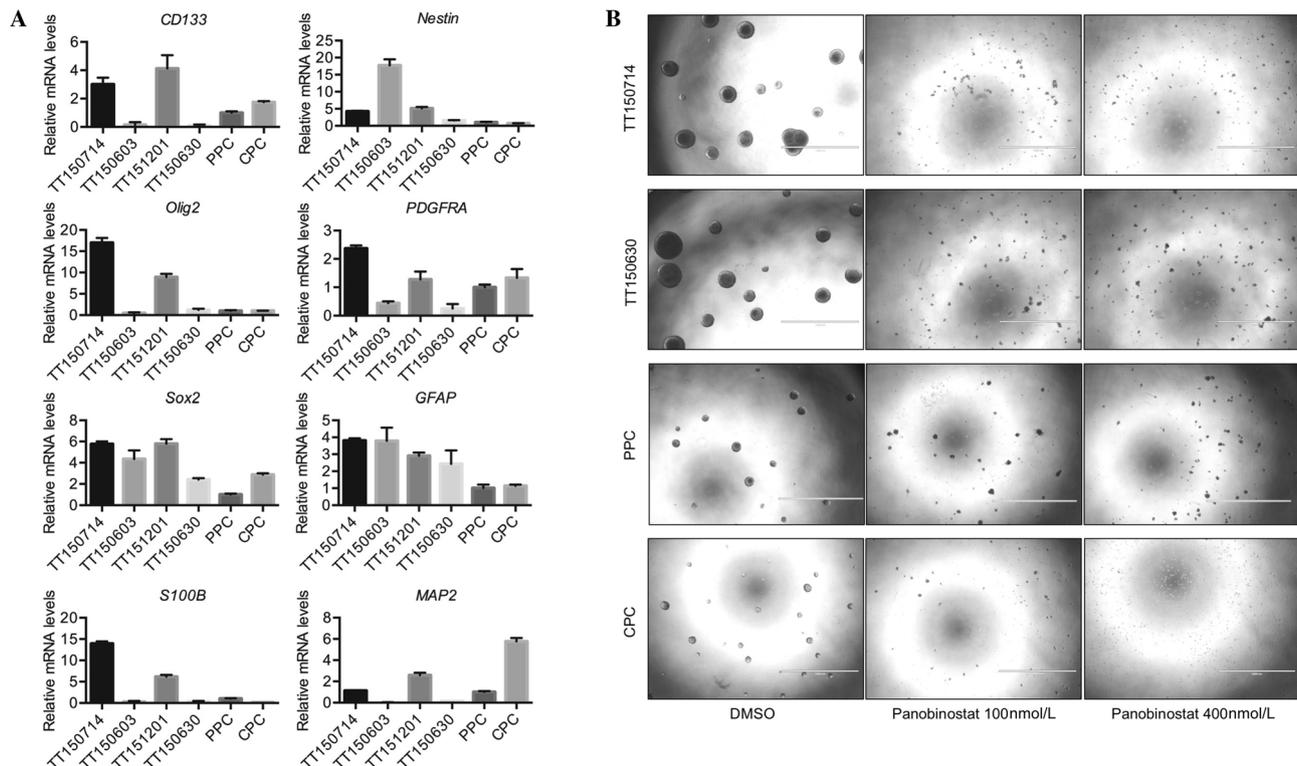
Fig. 3 DIPG cells, PPCs, and CPCs have similar molecular profiling and drug sensitivity. **A** The stem-cell markers CD133, Nestin, Olig2, PDGFRA, and Sox2 and the differentiation markers GFAP, S100B, and MAP2 analyzed by RT-PCR. **B** Representative images of sphere-forming assays showing similar drug sensitivity among DIPG cells, PPCs, and CPCs, 10 days after adding panobinostat at 100 nmol/L or 400 nmol/L, or 0.1% DMSO (3 replicates in each condition; scale bars, 1 mm).

H3K27M-transformed PPCs, proliferation and cell-cycle analysis also showed an increased Ki67-positive population and S-phase (Fig. 5C). Finally, RT-qPCR showed that the expression of *CD133* and *Sox2* was higher than in the empty vector (Fig. 5D). These data showed that PPCs obtained from the hindbrain of human fetuses can be immortalized by the DIPG-specific mutation H3K27M.

Validation of PPCs as Normal Controls for DIPG Cells

Ideal control cells for cancer research should have the potential to be used to dissect the molecular differences between normal and cancerous cells. In DIPG cells with the H3.3K27M mutation, the G1/S checkpoint pathway is highly enriched [20]. To validate the effectiveness of PPCs as normal control cells for DIPG cells, we compared the relative mRNA levels of typical G1/S checkpoint regulators in PPC and DIPG cell lines that harbored the H3.3K27M mutation. The *P53*, *P21*, and *P16* mRNA levels among DIPG cells were relatively lower than PPCs, providing direct evidence that the G1/S checkpoint dysregulation is common among DIPG cells (Fig. 6B).

Discussion

DIPG is the main cause of brain tumor-related death among children. Traditional radiotherapy and chemotherapy did not improve the overall survival for decades. Because of the infiltrative nature of the tumor and the deep, vital location of the pons, it has long been impossible to obtain tumor tissue for preclinical research. Until recently, with the development of minimally-invasive surgical techniques and primary culture methods, DIPG cell lines have been established from patient-derived DIPG tumor samples [3]. However, because of the vital physical functions of the pons, it is impossible to obtain para-tumor brain tissue as normal controls for DIPG cells. Dissecting the different molecular landscapes of tumor cells and corresponding normal cells is a powerful tool for identifying therapeutic targets for cancer. As a result, it is urgent to find normal control cells for DIPG cells to initiate preclinical research. Neural stem cells have characteristics in common with glioma stem cells to a great degree [4], making them potential candidates for normal controls for DIPG cells. Furthermore, neural stem cells induced from embryonic stem cells have also been reported to be able to model DIPG after transformation by oncogenes [5]. However,
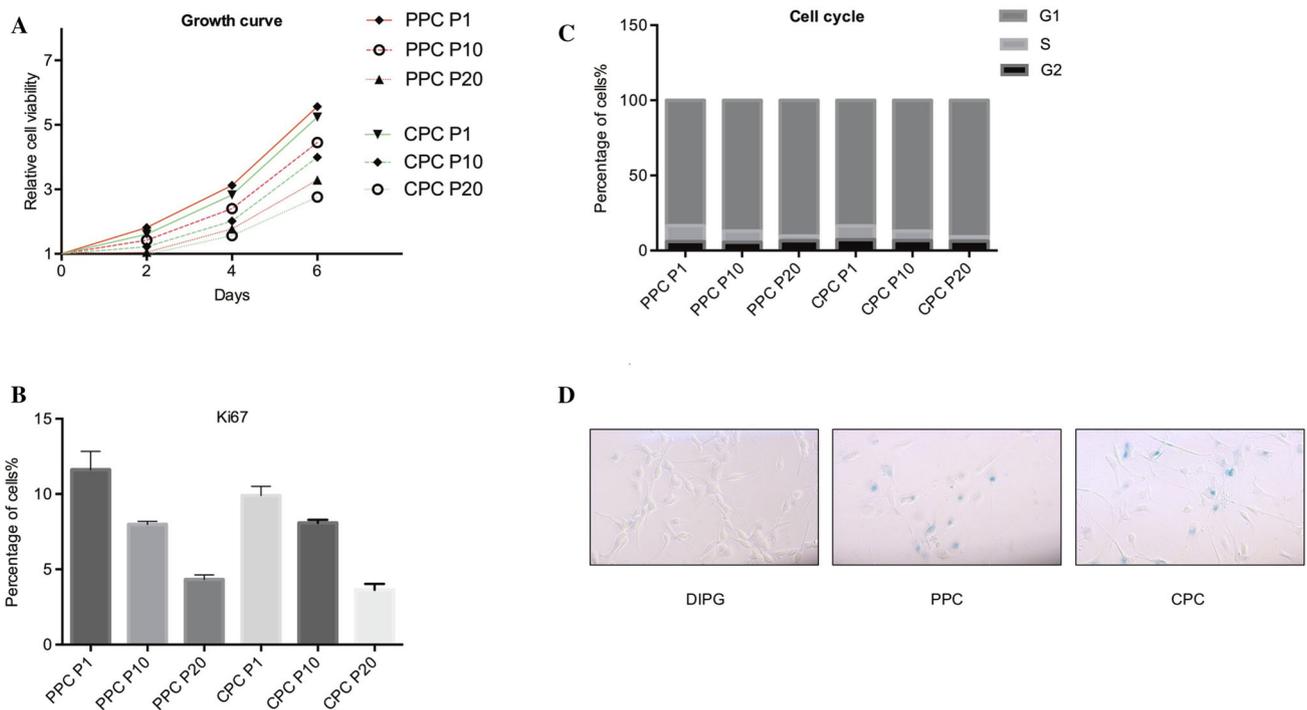
222

Neurosci. Bull. April, 2019, 35(2):216–224

Fig. 4 CPCs and PPCs derived from fetal brain demonstrated senescence after long-term passaging. **A** The growth rates of PPCs and CPCs decreased with passaging. **B** The Ki67-positive population declined with passaging. **C** The cell cycle-distribution showed a decrease in S-phase with passaging. **D** SA-β-Gal staining revealed that PPCs and CPCs suffered from senescence with passaging, but DIPG cells did not. P1, passage 1; P10, passage 10; P20, passage 20.
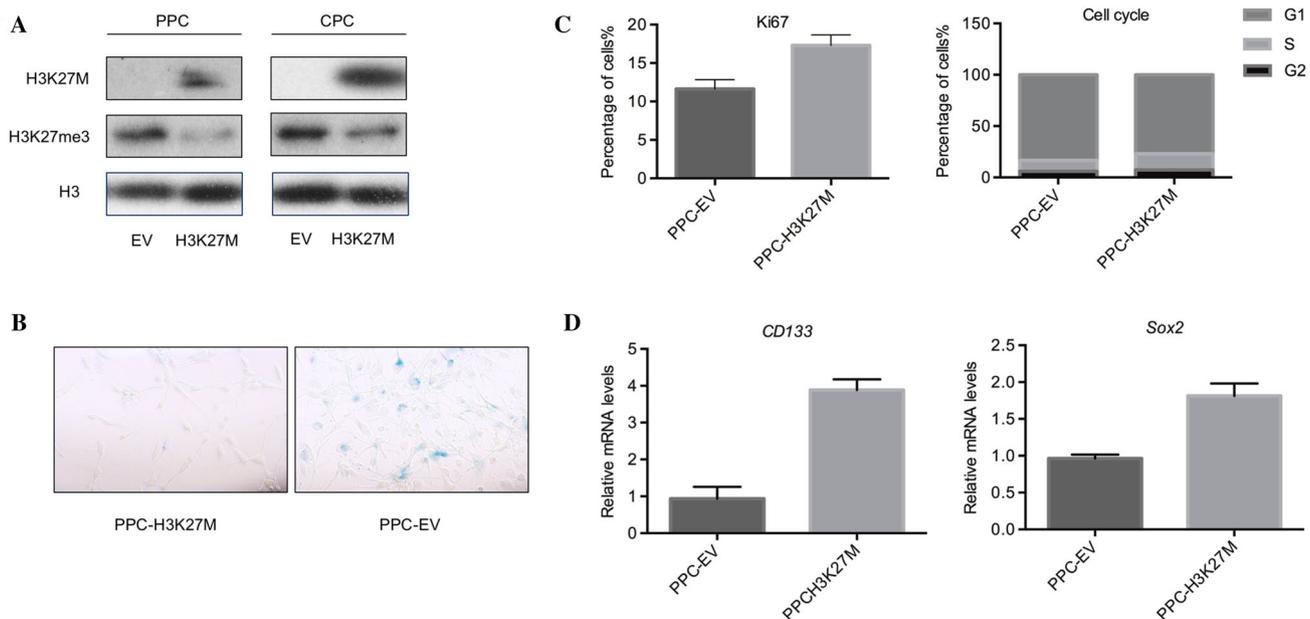

Fig. 5 PPCs transformed by the DIPG-specific H3K27M mutation became senescence-resistant. **A** Western blots showing that ectopic overexpression of the H3K27M mutation in PPCs decreased the global H3K27me3 level. **B** SA-β-Gal staining revealed that H3K27M mutation-transformed PPCs showed a smaller senescence population than PPCs overexpressing empty vector. **C** Left, Ki67 staining and flow cytometric analysis showing that PPCs transformed by H3K27M had higher proliferation than those with empty vector. Right, PI staining and flow cytometric analysis showing that the cell-cycle distribution of H3K27M-transformed PPCs had an increased S-phase distribution. **D** The mRNA expression levels of the stemness markers CD133 and Sox2 were higher in H3K27M-transformed PPCs.
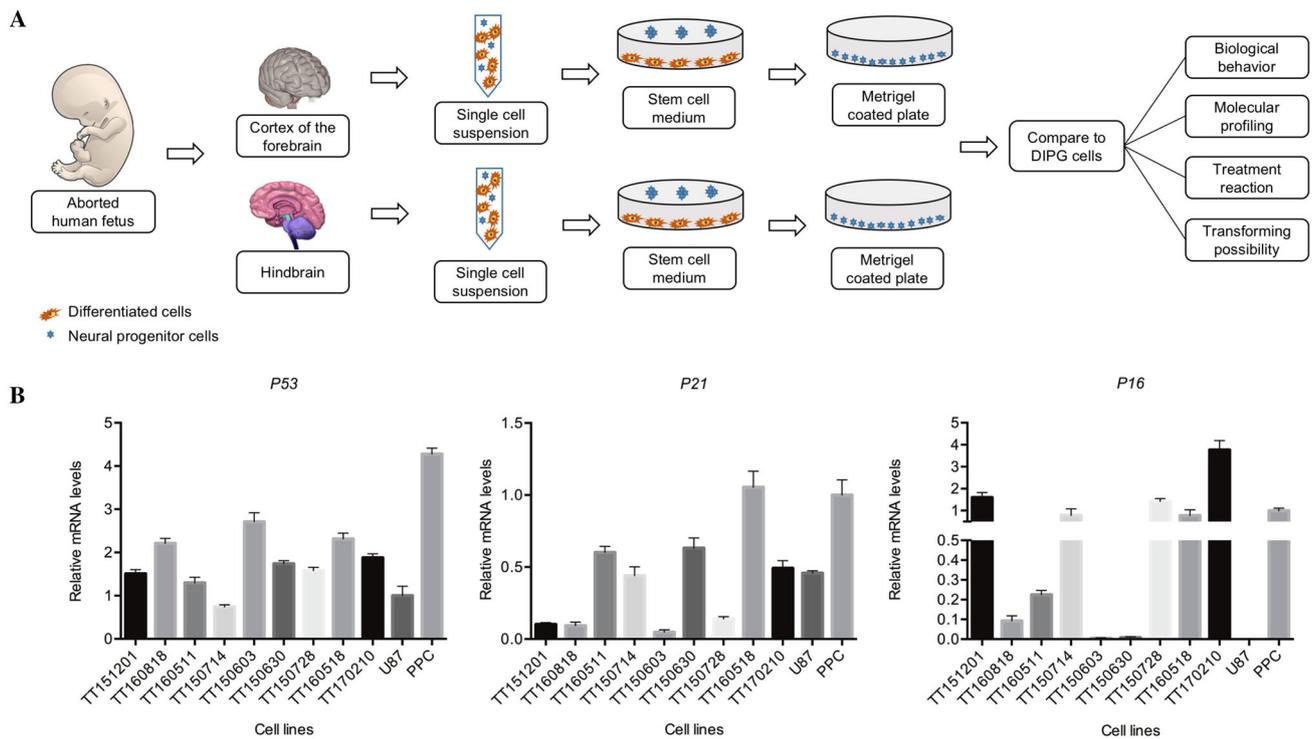
A

B

Fig. 6 Establishment and validation of PPCs as normal controls. **A** Flowchart for the establishment of neural progenitor cells from human fetal cortex and hindbrain. **B** Validation of PPCs as normal controls for DIPG cells. The relative mRNA levels of G1/S checkpoint regulators among primary DIPG cell lines harboring the H3K27M mutation (with initial TT) and the adult glioblastoma cell line U87 were compared to PPCs.

because of the spatial and temporal dynamics of the transcriptome in the central nervous system [7], it would be ideal to isolate NPCs from the pons as control cells for DIPG, which is thought to originate from pontine neural stem cells [3].

In this research, we provide a novel method to isolate and propagate NPCs derived from aborted human fetal brain and demonstrate that hindbrain-derived NPCs are ideal normal control cells for DIPG. First, we established primary DIPG cell lines from tumor tissue from treatment-naïve DIPG patients. Using various *in vitro* biological assays and *in vivo* tumor implantation assays, we verified that cancer stem cells were enriched in the DIPG cell lines. Second, we described a method of isolating NPCs from the brains of aborted human fetuses. Primary cells derived from the adult mouse brain form clusters of floating spheres in the presence of epidermal growth factor, demonstrating that neural stem cells are present in this cell population [21]. In this study, we demonstrated that both DIPG and primary cells derived from fetal brain contained cells that were able to form neurospheres. However, in the DIPG lines, single-cell sequencing revealed that H3K27M gliomas primarily contain cells that resemble oligodendrocyte precursor cells, while more-differentiated malignant cells are in a minority, which is different from the normal developmental process [22]. This was because the establishment of PPC and CPC cell lines involved processing of whole cortex and hindbrain, in which terminally-differentiated cells were the major population. This difference in the cellular architecture between DIPG and normal tissue further necessitated enrichment of NPCs by isolating neurospheres from the mixed population. After this enrichment, we demonstrated that both the CPCs and PPCs shared cell-biological and molecular signatures with cancer stem cells in DIPG, such as similar growth rates, cell-cycle distributions, proliferation markers, stemness markers, and differentiation markers.

As the numbers of passages increased, both the CPCs and PPCs began to show signs of senescence and decreased proliferation, but DIPG cells did not. One strategy to propagate NPCs *in vitro* is to overexpress oncogenes such as v-myc in the cells to achieve immortalization [18]. To test our hypothesis that specific DIPG driver mutation H3K27M would immortalize the NPCs derived from human fetuses, we overexpressed H3K27M in CPCs and PPCs. Surprisingly, this oncogene immortalized PPCs exclusively and not CPCs, which were not immortalized (data not shown). This result is consistent with the previous report that H3K27M expression in different cell contexts can induce senescence [5]. This mechanism would explain to some extent why another H3 mutation, H3G34R/V, frequently occurs within hemispheric glioblastomas in

224

Neurosci. Bull. April, 2019, 35(2):216–224

older patients, while the H3K27M mutation is specific to the pons [23]. The exclusively pontine H3K27M mutation allowed the NPCs in the pons (PPCs) to survive. However, NPCs originating in the hemispheres (CPCs) do not benefit from this cell-context-dependent oncogene overexpression.

Altogether, in this study we have provided a novel and simple method to isolate and enrich NPCs from aborted human fetal brain and revealed that DIPG cells exhibited cell-biological and molecular signatures of fetal hindbrain-derived NPCs. Thus, PPCs are desirable normal control cells for DIPG, and have the potential to model DIPG after transformed by DIPG-specific oncogenes. With the assistance of this tool, it will be possible to dissect the different responses of tumor cells and normal cells to multimodality therapies, including not only targeted pharmacological therapies [24] but also the physical therapies [25], and kill the tumor cells specifically without damage to normal cells. Besides functioning as normal controls for DIPG research, the application of PPCs may extend to the treatment of DIPG. For example, chemokines or growth factors released and expressed by glioma cells are able to mediate the tropism of stem cells in gliomas [26]. PPCs propagated and engineered *in vitro* could serve as candidate vehicles for various therapeutic agents, such as anti-tumor antibodies and cytokines, or even be used directly as subjects of cellular therapy.

Conflict of interest All authors claim that there are no conflicts of interest.

References

1. Maria BL, Rehder K, Eskin TA, Hamed LM, Fennell EB, Quisling RG, et al. Brainstem glioma: I. Pathology, clinical features, and therapy. J Child Neurol 1993, 8: 112–128.
2. Freeman CR, Perilongo G. Chemotherapy for brain stem gliomas. Childs Nerv Syst 1999, 15: 545–553.
3. Monje M, Mitra SS, Freret ME, Raveh TB, Kim J, Masek M, et al. Hedgehog-responsive candidate cell of origin for diffuse intrinsic pontine glioma. Proc Natl Acad Sci U S A 2011, 108: 4453–4458.
4. Lathia JD, Mack SC, Mulkearns-Hubert EE, Valentim CL, Rich JN. Cancer stem cells in glioblastoma. Genes Dev 2015, 29: 1203–1217.
5. Funato K, Major T, Lewis PW, Allis CD, Tabar V. Use of human embryonic stem cells to model pediatric gliomas with H3.3K27M histone mutation. Science 2014, 346: 1529–1533.
6. Chambers SM, Fasano CA, Papapetrou EP, Tomishima M, Sadelain M, Studer L. Highly efficient neural conversion of human ES and iPS cells by dual inhibition of SMAD signaling. Nat Biotechnol 2009, 27: 275–280.
7. Kang HJ, Kawasawa YI, Cheng F, Zhu Y, Xu X, Li M, et al. Spatio-temporal transcriptome of the human brain. Nature 2011, 478: 483–489.
8. Tailor J, Kittappa R, Leto K, Gates M, Borel M, Paulsen O, et al. Stem cells expanded from the human embryonic hindbrain stably retain regional specification and high neurogenic potency. J Neurosci 2013, 33: 12407–12422.
9. Xu C, Liu X, Geng Y, Bai Q, Pan C, Sun Y, et al. Patient-derived DIPG cells preserve stem-like characteristics and generate orthotopic tumors. Oncotarget 2017, 8: 76644–76655.
10. Shechter D, Dormann HL, Allis CD, Hake SB. Extraction, purification and analysis of histones. Nat Protoc 2007, 2: 1445–1457.
11. Ignatova TN, Kukekov VG, Laywell ED, Suslov ON, Vrionis FD, Steindler DA. Human cortical glial tumors contain neural stem-like cells expressing astroglial and neuronal markers in vitro. Glia 2002, 39: 193–206.
12. Bender S, Tang Y, Lindroth AM, Hovestadt V, Jones DT, Kool M, et al. Reduced H3K27me3 and DNA hypomethylation are major drivers of gene expression in K27M mutant pediatric high-grade gliomas. Cancer Cell 2013, 24: 660–672.
13. Gotz M, Huttner WB. The cell biology of neurogenesis. Nat Rev Mol Cell Biol 2005, 6: 777–788.
14. Li Z, Wang H, Eyler CE, Hjelmeland AB, Rich JN. Turning cancer stem cells inside out: an exploration of glioma stem cell signaling pathways. J Biol Chem 2009, 284: 16705–16709.
15. Yan K, Wu Q, Yan DH, Lee CH, Rahim N, Tritschler I, et al. Glioma cancer stem cells secrete Gremlin1 to promote their maintenance within the tumor hierarchy. Genes Dev 2014, 28: 1085–1100.
16. Grasso CS, Tang Y, Truffaux N, Berlow NE, Liu L, Debily MA, et al. Functionally defined therapeutic targets in diffuse intrinsic pontine glioma. Nat Med 2015, 21: 555–559.
17. Wright LS, Prowse KR, Wallace K, Linskens MH, Svendsen CN. Human progenitor cells isolated from the developing cortex undergo decreased neurogenesis and eventual senescence following expansion in vitro. Exp Cell Res 2006, 312: 2107–2120.
18. Ryder EF, Snyder EY, Cepko CL. Establishment and characterization of multipotent neural cell lines using retrovirus vector-mediated oncogene transfer. J Neurobiol 1990, 21: 356–375.
19. Piunti A, Hashizume R, Morgan MA, Bartom ET, Horbinski CM, Marshall SA, et al. Therapeutic targeting of polycomb and BET bromodomain proteins in diffuse intrinsic pontine gliomas. Nat Med 2017, 23: 493–500.
20. Mackay A, Burford A, Carvalho D, Izquierdo E, Fazal-Salom J, Taylor KR, et al. Integrated molecular meta-analysis of 1,000 pediatric high-grade and diffuse intrinsic pontine glioma. Cancer Cell 2017, 32: 520–537 e525.
21. Reynolds BA, Weiss S. Generation of neurons and astrocytes from isolated cells of the adult mammalian central nervous system. Science 1992, 255: 1707–1710.
22. Filbin MG, Tirosh I, Hovestadt V, Shaw ML, Escalante LE, Mathewson ND, et al. Developmental and oncogenic programs in H3K27M gliomas dissected by single-cell RNA-seq. Science 2018, 360: 331–335.
23. Schwartzentruber J, Korshunov A, Liu XY, Jones DT, Pfaff E, Jacob K, et al. Driver mutations in histone H3.3 and chromatin remodelling genes in paediatric glioblastoma. Nature 2012, 482: 226–231.
24. Shi Y, Guryanova OA, Zhou W, Liu C, Huang Z, Fang X, et al. Ibrutinib inactivates BMX-STAT3 in glioma stem cells to impair malignant growth and radioresistance. Sci Transl Med 2018, 10. pii: eaah6816.
25. Zeng Y, Shen Y, Hong L, Chen Y, Shi X, Zeng Q, et al. Effects of single and repeated exposure to a 50-Hz 2-mT electromagnetic field on primary cultured hippocampal neurons. Neurosci Bull 2017, 33: 299–306.
26. Xu F, Zhu JH. Stem cells tropism for malignant gliomas. Neurosci Bull 2007, 23: 363–369.